

A7: Distribution of Electric Charges on a Disc

Jake Pommills

School of Physics and Astronomy, University of Southampton, Southampton, UK

Abstract — A 2D variation of Thomson’s problem[1] has been investigated, and we have verified results by Wille and Vennik (1985). Configurations with the smallest electrostatic potential energy of N charges bounded to a disc is found for $2 - 30(+)$ charges. Different regions have been found and displayed which defines the behaviour of charges within a disc, which appear to form concentric rings of charges around the disc.

I. INTRODUCTION

In order to investigate The Plum Pudding Model further, J.J. Thomson proposed a problem in 1904, which had the objective to find the minimum electrostatic potential energy of N similarly charged particles, on the surface of a sphere. This is equivalent to Smale’s 7th problem[2] which remains unsolved, so numerical methods must be used. We investigate a similar problem; proposed by Berezin[3], pertaining to a disc, and allowing charges to exist anywhere on the disc, and not just on its perimeter.

We know intuitively that N similar charges will repel each other and for a small N , we can guess that these charges lie on the boundary of the disc. However all the space on the disc is available, and as N becomes larger, we would expect charges to utilise this space better to reduce the potential energy. Where this changeover occurs, between configurations where charges only exist on the circumference, and configurations with charges free from the circumference is to be determined, along with the properties and formations of these configurations should be investigated.

This problem is made computationally tough by the fact that (for sufficient N) there are several minima, that is to say there are many non-congruent configurations of charges such that no allowed change δx or δy on any charge will decrease the electrostatic potential. This NP problem can be tackled with a method of simulated annealing, suggested by Wille and Vennik[4]. They introduce the idea of a temperature to the system which allows the program to jump/escape from these electrostatic potential minima, and find the absolute minimum of electrostatic potential.

II. THEORY & BACKGROUND

We are trying to find the minimum electrostatic potential energy of the system, so we must have some equation to calculate this potential energy. This equation for computing the energy of N similar charges is given by

$$W_{ij} = \frac{q^2}{2R} \sum_{i,j}^{i \neq j} \frac{1}{|\mathbf{r}_i - \mathbf{r}_j|} \quad (1)$$

where $\mathbf{r}_i, \mathbf{r}_j$ is the position of the i th, j th charge, and R is the radius of the disc. As charges are similar, and the radius of the disc is independent of the charges, we may take them out of the sums. In this report, $W_{ij} = W$ and will be quoted in terms of q^2/R . A factor of $1/2$ appears in the formula as we wish to not double-count distances (such as R_{21} and R_{12})

The algorithm we follow each iteration of the program is as follows:

- Choose a charge at random.
- Choose either the x or y coordinate at random.
- Increase or decrease randomly the coordinate by a small fixed length δ .
- Compute the change in energy ΔW that results.
- If the energy decreases accept the change in the coordinate.
- If the energy increases then accept the change with a probability proportional to $\exp(\Delta W/T)$.

The general idea of the algorithm is to try a new (albeit very similar) configuration of the charges and find out if it has a lower potential energy. When the program finds a more favourable position, it will change to it and then repeat.

This algorithm has an objective to solve a problem which we know can fall into multiple stable configurations, so some way of getting out of these stable configurations to other stable configurations, which may have lower electrostatic potential are required. We introduce the concept of temperature into the system to solve this problem. We impose the last condition onto the algorithm, and actually allow the system to change into a higher W state, with a temperature dependant probability $p(\Delta W, T)$. If we reduce T periodically, we allow the program to escape smaller stable configurations, and find itself with a configuration close to the best configuration; by which time the temperature will have decayed sufficiently that

further iterations will only bring the configuration down the well, and then show us the best configuration.

Our program uses the statement that T should be decreased to $0.9T$ every 100 iterations (We choose the values 0.9 and 100, similarly used by Wille and Vennik), then we have

$$T = T_{init} \cdot 0.9^{\lfloor i/100 \rfloor} \quad (2)$$

where i is the number of iterations. If we then combine this with our probability function stated in our algorithm, we find

$$p(\Delta W, i) = \exp(-\Delta W / T_{init} \cdot 0.9^{\lfloor i/100 \rfloor}) \quad (3)$$

$p(\Delta W, i)$ plotted against i is like a discrete decay shown in Figure 2 (Note that this probability function is only relevant for $\Delta W > 0$, so it is acceptable that the function blows up for positive ΔW) We see that with a large amount of iterations, the probability function drops to zero, and (if $T \gg 0$) the function is unity when the system has just started evolving.

The initial temperature changes how long a system can exist in an “excited state”, that is to say a state where the system is accepting any change. It is during these iterations that the algorithm can escape local minima. Choosing an appropriate T_{init} is dependant on the size of N , as in general higher N systems have more local minima which we want to avoid.

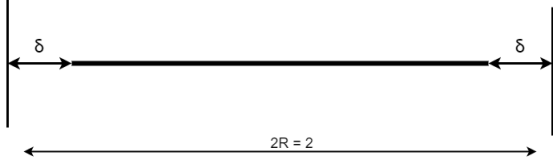


Fig. 1: Worst case scenario for errors for $N = 2$

The program only allows a shift in \hat{x} or \hat{y} in one iteration. This means our shift amount, δ is going to define the “worst case error”. Taking the $N = 2$ system as an example, we can demonstrate this worst case error on a line (after many iterations), shown in figure 1. Since charges are generated randomly, they will end up in a position between the edge of the boundary and the boundary edge $+\delta$. We therefore take the max error for the distance between two charges is 2δ . This is also similar to having a smaller radius of $1 - \delta$. When calculating W , this will look like

$$W = \frac{1}{2 - 2\delta} = \frac{1}{2(1 - \delta)} = \frac{1}{2} \frac{1}{R_\delta} \quad (4)$$

Where $R_\delta = 1 - \delta$ and worst case error can be calculated with this factor. Extending this to $2D$, The same scheme where the error is given by $1/R_\delta$. As our computed W values are

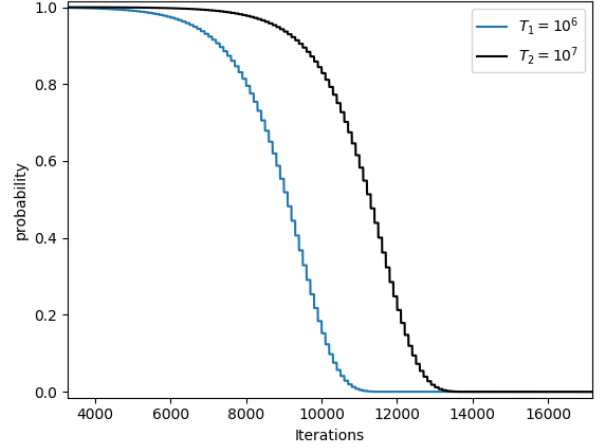


Fig. 2: Discrete exponential decay model of the probability distribution function at two temperatures T_1 and T_2 . (In the real system ΔW will not be constant across iterations)

in units of q^2/R , we may multiply theoretically calculated W values by $1/R_\delta$ to find the range of W that represents the range of W values that correspond to the best configuration.

III. RESULTS

A computational implementation of computing a W value, and a program performing our previously stated algorithm has been built in Python, in order to find the minimum potential energies.

TABLE I

Shape (Regular)	N	Theoretical W	Computed W
Line	2	0.5000	0.5001
Triangle	3	1.7321	1.7333
Square	4	3.8284	3.8299
Pentagon	5	6.8819	6.8891
Hexagon	6	10.9641	10.9753
Heptagon	7	16.1334	16.1553
Octagon	8	22.4389	22.5041
Nonagon	9	29.9234	30.0207
Decagon	10	38.6245	38.7515
Hendecagon	11	48.5757	48.7565
Dodecagon	12	59.8074	59.7644

A. Circumference Charges

In Figure 9, we present visuals of best configurations found from 2 charge systems to 12 charge systems. In Table I, we show the computed values for W , and contrast it to the theoretical lowest electrostatic potential produced with the same amount of charges, of different regular shapes inscribed in a circle of unit radius. Graphically, we can show this in Figure 3,

which plots the difference of computed and theoretical energy values. We would expect from the graph that for all $N \geq 12$, W_{theory} stops having any meaning as every configuration will not abide by its initial assumption (that all charges lie on the circumference). Appendix A shows how some of these theoretical calculations of shapes were found. It is impossible to get a lower W than the W_{theory} values tabulated here, with the condition that all charges must be on the circumference - except we find that for $N = 12$, the computed W is lower than the circumference theory W value, and we can see the obvious difference in the graphical representation. This result for changeover at $N = 12$ is strongly linked to the formula $W \propto 1/R$ [5]

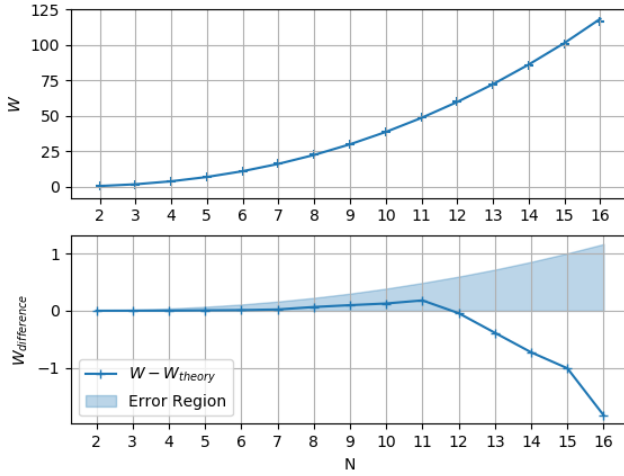


Fig. 3: (Top) A plot showing the apparent exponential increase of our found W values against N . (Bottom) A plot displaying the error region calculated from multiplying W_{theory} by the worst case radius correction, $1/(1 - \delta)$.

We see that the theory of circumference charges departs from reality at $N = 12$, but there is no visual difference or shift in the actual W value. Computed values for $N \geq 13$ were included in the plot to demonstrate the increasing negative difference in W

B. 1st Ring Charges

For charges $N \geq 12$, we find minimal energy solutions that have configurations with charges not on the circumference. In Figures 10 and 11, we observe that minimum configurations seem to repeat the amount of non-circumference charges, and some “inner ring” forms. We can tabulate the average radius of this new ring, and how many charges lie on this new ring. When there is one ring or more present, the possible numbers of local minima is greatly increased[6], which increases the difficulty in achieving solutions.

C. 2nd Ring Charges & Beyond

After $N = 30$, a new central charge emerges, and beyond that, more properties of the whole system become more clear. Charges can now land on the circumference, or the first ring, and expand the innermost ring. We may expect this behaviour to continue and many more rings will appear on the disc.

In Table II, We have tabulated results for W , and written their apparent configuration, and the average radius produced by charges. The trend of W is continues from the results of Table I. Our tabulated configurations match results obtained by Nurmela (1997).

Included is $N = 55$ and $N = 56$, which is the expected changeover region given by Nurmela. We find graphically that $N = 56$ is the next magic number in the series, giving rise to the next ring.

TABLE II

N	W	Configuration	r_{ring}
13	71.9611	12 1	-
14	85.4936	13 1	-
15	100.4452	14 1	-
16	116.6236	15 1	-
17	134.0794	15 2	0.3331
18	152.8834	16 2	0.3301
19	172.9075	16 3	0.4041
20	194.0892	17 3	0.3980
21	216.7637	18 3	0.3890
22	240.7594	18 4	0.4379
23	266.1548	19 4	0.4351
24	292.4273	20 4	0.4300
25	321.0215	20 5	0.4727
26	349.8462	21 5	0.4650
27	380.6980	21 6	0.5012
28	412.8701	22 6	0.4937
29	444.7493	23 6	0.4882
30	480.5790	23 6 1	0.4739
55	1801.4924	38 12 6	0.5258
56	1874.0275	38 12 6 1	0.5121

The average radius of these charges might have no apparent pattern, but if plotted (Figure 4), and also display the regions of different numbers of inner circle charges, we can see adding charges to the newest ring will jump the radius up, but adding a charge to the circumference (an outer ring) will decrease the radius. We expect this trend to continue with further amounts of rings, but will have more complex situations as charges can have more than one other ring to land on.

IV. DISCUSSION

For further computations of higher N values, it would be valuable to rewrite code in a compiled language, (such as C

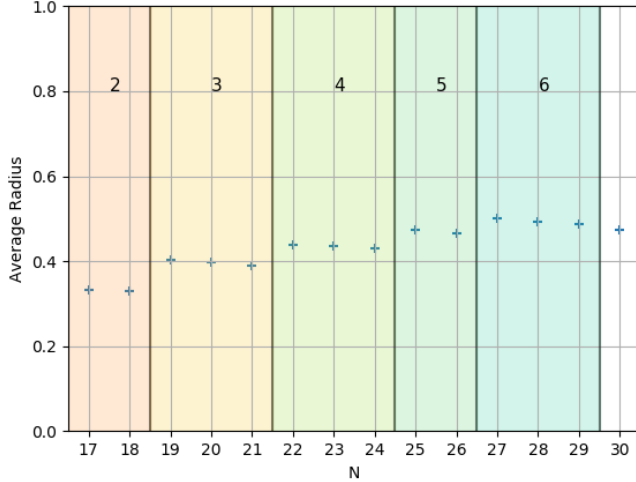


Fig. 4: Plot of the average radius against number of charges. The labeled regions refer to the number of charges in the outer ring. We note that adding charges to the newest ring will jump the radius up, but adding a charge to the circumference will decrease the radius. The general trend is increasing.

or Fortran) due to the non-linear increases in time complexity of the program. Improvements were made to reduce time complexity when it was needed. (such as an improved way of computing W) However for this use case, Python was satisfactory for $N \leq 30$.

There are other methods other than simulated annealing, which has been used to solve similar problems. Almost all techniques to solve this problem[4], [7], [8] (Including simulated annealing) fall into the bracket of “Stochastic optimisation”. These optimisation methods are particularly suited for this problem because a global minima is needed when there are several local minima. There have been instances since Berezin’s proposal where a believed global minima has been wrong, and is later corrected.[5] This is the case for $N = 17$ and $N = 23$, where the actual global minimum had a different amount of central charges shown in Figure 5. This further emphasises the need for simulated annealing to get over these non-global minima, and also find the right initial conditions for temperature and how the temperature decreases.

3D versions of this problem can be studied, and through a review, there appears to be more research on this variation of the problem, likely due to the physical relevance of 3D variations on this problem. That is not to say that 2D variations are not physically relevant, as Berezin’s initial proposal came from interest in the structure of snowflakes[9]. It appears many of the difficulties of 2D problems are translated into similar 3D problems too, so tools and techniques used to tackle the

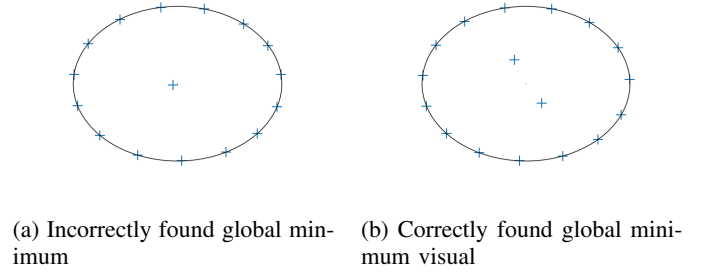


Fig. 5: $N = 17$

2D problem should be able to help similar 3D problems too. Tackling the easier 2D problems first is then very valuable, as less effects are at play, and what techniques perform well or poor can be determined quicker.

It was hoped that there would be some powerful predictive power that emerged from the ring patterns beyond one ring. It was found that for 1st ring charges, if the solution for N and $N+2$ had the same amount of inner ring charges, then it could be determined what the $N+1$ solution would look like. see Figure 10 (h)-(j). If (h) and (j) are known, then we can know that (i) will add a charge to the circumference. Unfortunately this fact existing for range $N = 12 - N = 30$ does not hold when there are further rings. As computation gets more difficult with increasing N , any form of deterministic prediction would be very valuable and this concept should be explored further. There is one hypothesis that emerges when we assume the ring formations continues infinitely, and that is “The best written configuration $N+1$ will not have more than one difference than the best written configuration N ” This means that when one more charge is introduced, only one ring will actually change and receive one more charge (or make a new ring). This hypothesis holds true for the computed values in this report, and also holds for the findings of Nurmela (1997). If this is true, we can use this to be able to reject some local minima if the previous configuration global minima is known, and 2 or more rings have been perturbed.

V. CONCLUSION

We have computed minimum electrostatic potential energies W , along with visual representations, for N charges confined to a 2D disc, and found many of the expected properties of ring formations that these systems will fall into, and how more rings appear, by slowly pushing the innermost ring towards the circumference of the disc, to make room for a new ring. We have found three magic numbers, $N = 12, 30, 56$ which correspond to an increase in the number of rings present on the disc.

We have discussed the implications of if the ring formations continuing indefinitely, and also possible time-saving techniques are suggested.. We have shown possible local minima that our program could have fallen into but avoided - giving legitimacy to the use of simulated annealing with this problem. Our report has shown this approach can be implemented in faster languages to larger scale problems (such as Thomson's problem) in 3D, with similar success to problems in 2D, or to calculate further N values in regard to the 2D disc problem.

APPENDIX

To solve the problems in the table, we use a unit circle, inscribed with regular shapes we are investigating. We look at the distances from one charge to all the others; which a theoretical W can be computed from:

In all cases, we can exploit rotational symmetry of the circle, so that we can compute the distances of one charge, and then multiply by N , the number of charges.

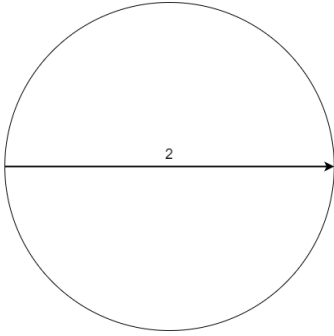


Fig. 6: Line inscribed in a circle.

For figure 6, we see the distance is 2, and we can plug into the formula for W_{ij}

$$W_{N=2} = \frac{1}{2} \left[2 \frac{1}{2} \right] = 0.5 \quad (5)$$

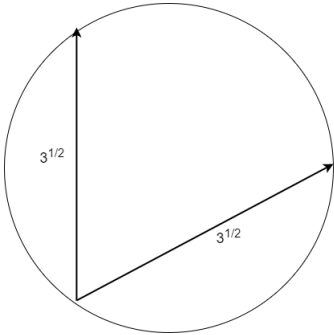


Fig. 7: Points of an equilateral triangular inscribed in a circle.

For figure 7, we see the distances to both charges are $\sqrt{3}$ (by construction), and we can plug into the formula for W_{ij}

$$W_{N=3} = \frac{1}{2} \left[3 \left(\frac{2}{\sqrt{3}} \right) \right] = \sqrt{3} \approx 1.7321 \quad (6)$$

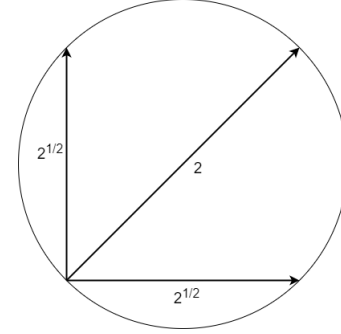


Fig. 8: Points of square inscribed in a circle.

For figure 8, we compute $W_{N=4}$ in the same way as previously.

$$W_{N=4} = \frac{1}{2} \left[4 \left(\frac{1}{2} + \frac{2}{\sqrt{2}} \right) \right] = 1 + 2\sqrt{2} \approx 3.8284 \quad (7)$$

For $N > 5$, a one-by-one approach becomes tedious, so a generic solution from the cosine rule with two lengths in a circle of unit radius is constructed for any N which is as follows:

$$D_m = \sqrt{2 - 2\cos(Im)} \quad (8)$$

where D_m is the distance between two points, I is the interior angle of the shape inscribed in the circle, and m is an integer such that $Im > 2\pi$. We can then exploit this, and rotational symmetry to find a formula

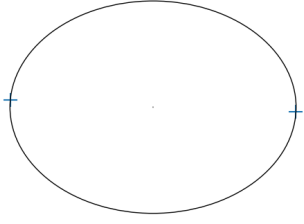
$$W_{theory} = N \sum_m \frac{1}{D_m} \quad (9)$$

Which makes finding W_{theory} easily computable. Code for computing W_{theory} is provided.

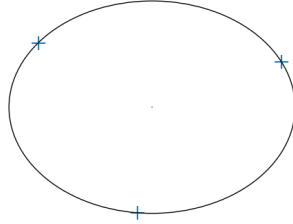
REFERENCES

- [1] J. J. Thomson, "On the structure of the atom: An investigation of the stability and periods of oscillation of a number of corpuscles arranged at equal intervals around the circumference of a circle; with application of the results to the theory of atomic structure," *Phil. Mag*, vol. 7, no. 39, pp. 237–265, 1904. DOI: 10.1080/14786440409463107.

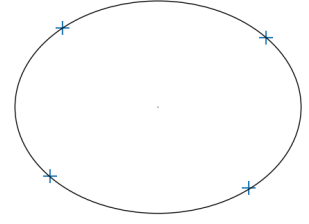
- [2] S. Smale, “Mathematical problems for the next century,” *The Mathematical Intelligencer*, vol. 20, no. 2, pp. 7–15, Mar. 1998, ISSN: 0343-6993. DOI: 10.1007/BF03025291.
 - [3] A. A. Berezin, “An unexpected result in classical electrostatics,” *Nature*, vol. 315, p. 208, May 1985. DOI: 10.1038/317208c0.
 - [4] L. T. Wille and J. Vennik, “Electrostatic energy minimisation by simulated annealing,” *Journal of Physics A: Mathematical and General*, vol. 18, no. 17, pp. L1113–L1117, Dec. 1985. DOI: 10.1088/0305-4470/18/17/009.
 - [5] M. G. Calkin, D. Kiang, and D. A. Tindall, “Minimum-energy charge configurations,” *American Journal of Physics*, vol. 55, no. 2, pp. 157–158, 1987. DOI: 10.1119/1.15235.
 - [6] P. Amore and M. Jacobo, “Thomson problem in one dimension: Minimal energy configurations of n charges on a curve,” *Physica A: Stat. Mech. and its Applications*, vol. 519, pp. 256–266, 2019, ISSN: 0378-4371. DOI: <https://doi.org/10.1016/j.physa.2018.12.040>.
 - [7] K. J. Nurmela, “Minimum-energy point charge configurations on a circular disk,” *Journal of Physics A: Mathematical and General*, vol. 31, no. 3, pp. 1035–1047, Jan. 1998. DOI: 10.1088/0305-4470/31/3/014.
 - [8] L. T. Wille, “Searching potential energy surfaces by simulated annealing,” *Nature*, vol. 324, pp. 46–48, Nov. 1986. DOI: 10.1088/0305-4470/18/17/009.
 - [9] W. S. Mortley, “An unexpected result in classical electrostatics,” *Nature*, vol. 313, p. 638, Feb. 1985. DOI: 10.1038/317208c0.
-



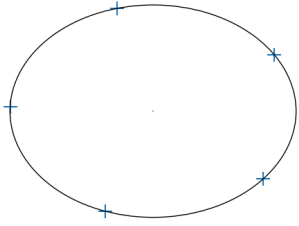
(a) $N = 2$



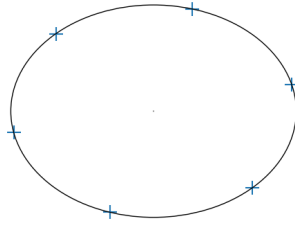
(b) $N = 3$



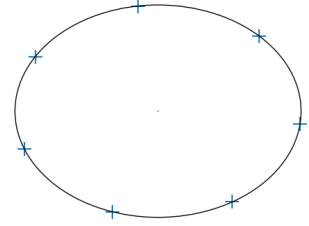
(c) $N = 4$



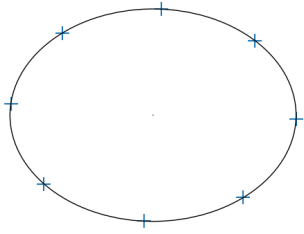
(d) $N = 5$



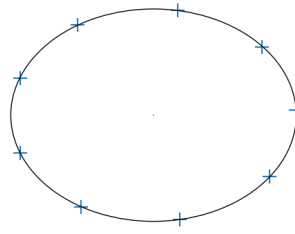
(e) $N = 6$



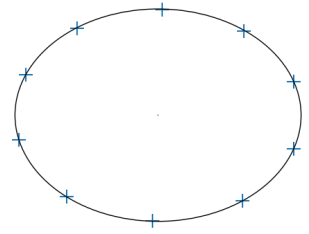
(f) $N = 7$



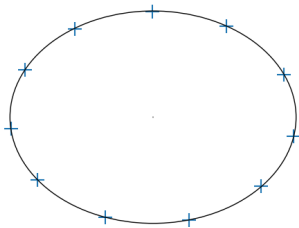
(g) $N = 8$



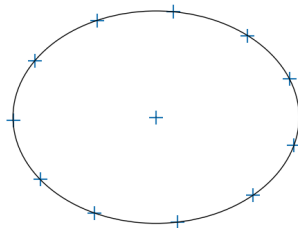
(h) $N = 9$



(i) $N = 10$

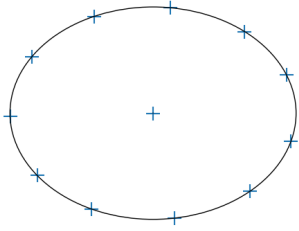


(j) $N = 11$

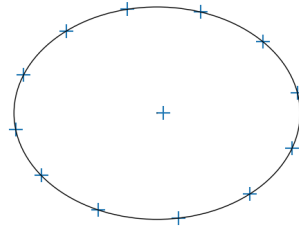


(k) $N = 12$

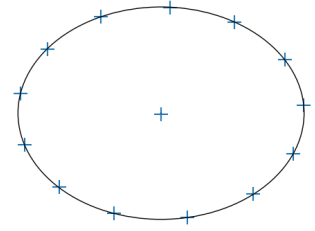
Fig. 9: Graphical representations of our simulation $N = 2 - N = 12$. We can easily identify a change in regime between (j)-(k). [Each produced with 10^6 iterations, $\delta = 0.01$, and the computed W value is quoted in Table I]



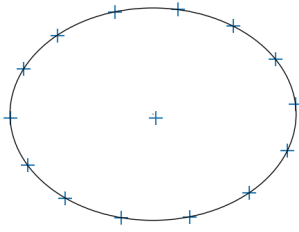
(a) $N = 12$



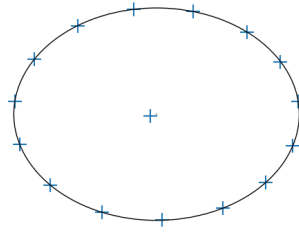
(b) $N = 13$



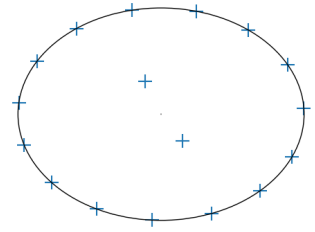
(c) $N = 14$



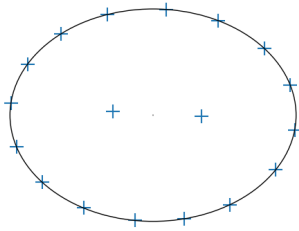
(d) $N = 15$



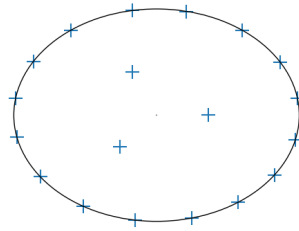
(e) $N = 16$



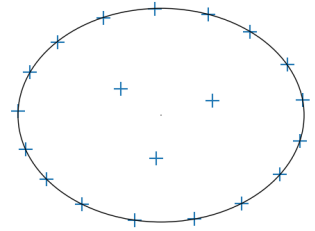
(f) $N = 17$



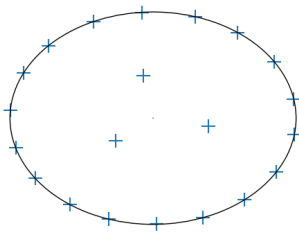
(g) $N = 18$



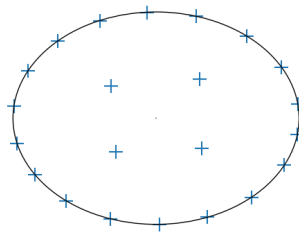
(h) $N = 19$



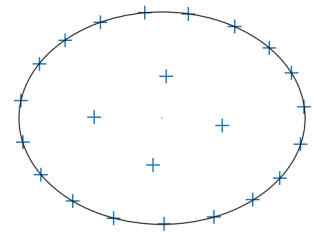
(i) $N = 20$



(j) $N = 21$

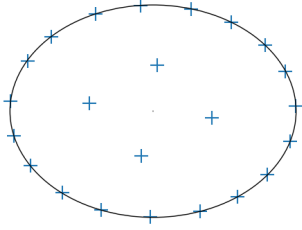


(k) $N = 22$

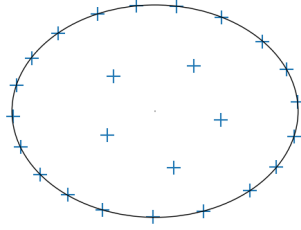


(l) $N = 23$

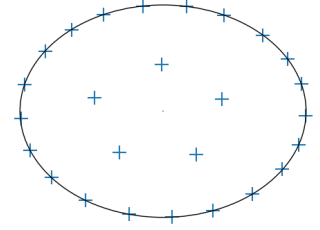
Fig. 10: Graphical representations of our simulation $N = 12 - N = 23$. [Each produced with 10^6 iterations, $\delta = 0.01$, and the computed W value is quoted in Table II]



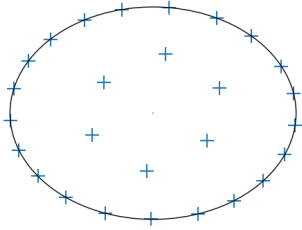
(a) $N = 24$



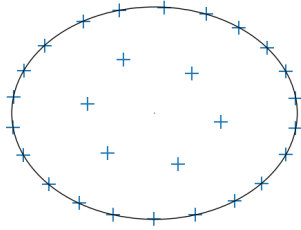
(b) $N = 25$



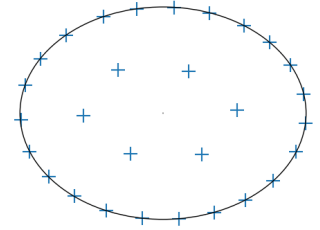
(c) $N = 26$



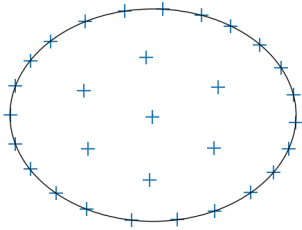
(d) $N = 27$



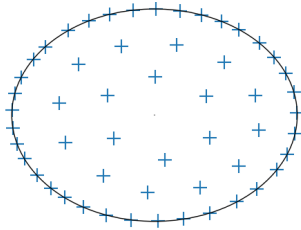
(e) $N = 28$



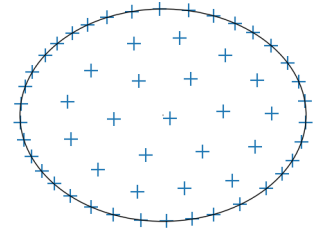
(f) $N = 29$



(g) $N = 30$



(h) $N = 55$



(i) $N = 56$

Fig. 11: Graphical representations of our simulation. $N = 24 - N = 30$, and $N = 55, 56$. [Each produced with 10^6 iterations, $\delta = 0.01$, and the computed W value is quoted in Table II] (except (h), (i), produced with 2.5×10^5 iterations.)]